17th World Conference on Earthquake Engineering, 17WCEE

Sendai, Japan - September 13th to 18th 2020

COMPONENT RESPONSE OF BASE ISOLATED STRUCTURE UNDER SEISMIC EXCITATION

S. Chakraborty(1), S. Ray-Chaudhuri(2)

(1) Assistant Professor. Civil Eng., Indian Institute of Technology Palakkad, India, E-mail: sanjukta@iitpkd.ac.in
(2) Professor, Dept. of Civil Eng., Indian Institute of Technology Kanpur, India, E-mail: samitrc@iitk.ac.in

Abstract

In this study, an experimental investigation is carried out to assess the seismic design requirements for SDOF nonstructural components attached to a primary structure, which is undergoing nonlinear hysteretic-type force deformation behavior. The purpose of adding the component is two-fold: (i) to verify the excitation of higher modes as a result of change in stiffness of the primary structure as is reported by a recent study and (ii) to estimate the component response amplification under such circumstances. In order to simulate the hysteretic behavior of the primary structure, three base conditions such as fixed, sliding and sliding with nonlinear spring are considered. Two types of components are considered: i) components tuned to the fundamental mode of the primary structure and ii) components tuned to the second mode of the primary structure. Shake table experiments are conducted with a scaled model of a single bay, three-story moment-resisting steel frame structure. The amplification in the component responses tuned to the different modal frequencies (different component types) of the primary structures are estimated for different base conditions. Additionally, the amplification in the component responses attached to a particular floor level of the primary structure is evaluated with respect to the horizontal peak floor acceleration corresponding to that particular floor level for all the base conditions and such amplification is compared with the component amplification factor as specified in codal provisions. From the recorded floor accelerations and component acceleration responses, it is observed that indeed higher modes show more energy content after a sudden change in stiffness of the structure as a result of sudden sliding. This phenomenon amplifies the component response significantly as compared to the fixed base structure. Moreover, it is found from the study that the code specified factor for the component amplification underestimates the actual component amplification that occurs due to the sudden change in the stiffness of the structure.

Keywords: component response, attached components, base isolated system, higher mode excitation, energy transfer

1. Introduction

Base isolation is one of the most popular strategies to control response of structures under seismic excitation. The popularity is obvious from an increasing number of structures being isolated seismically world-wide. Base isolation can reduce or limit the force transferred to the superstructure during severe earthquakes and hence, a structure can be protected from the devastating effect of ground excitations without increasing the capacity of different structural elements. The development in this area is obvious from a large number of studies, highlighting the conceptual and experimental works. There are different types of base isolation systems such as, spring associated with a damper as in the case of a laminated or lead rubber bearing or a sliding base isolation system as in case of a fat sliding isolator or friction pendulum [1]. Flat sliding isolator makes a structure insensitive to the intensity of base shaking and the frequency content of the ground motion, since the force transfer from the ground to the super-structure is capped by the frictional force during its sliding phase. Furthermore, these bearings provide dissipation of the seismic energy due to friction mechanism. However, sliding type isolation results into a huge base and residual displacements of the structures. In order to overcome this drawback, various restoring devices are invented such as the friction pendulum system [2, 3, 4, 5, and 6] and isolation with linear and angular springs [7]. In a recent study [8] by the authors of this paper, an adaptive base isolation system considering a flat sliding isolator coupled with a conical spring is considered. The system is found to be very effective in reducing the base and residual displacement without hampering the efficiency of base isolation. However, such sliding can be detrimental to the attached nonstructural components of a primary structural system. This is because a sudden change in the stiffness of the structure causes significant energy transfer to the higher modes of the structural system as shown in another work of these authors [9]. This is particularly important when the frequency of a component is tuned to the higher modes of the structure on which the component is attached. Hence, seismic vulnerability of such a component may be higher in base isolated structure in comparison to the same component housed in the same structure but fixed at base.

In this paper, the component excitation that takes place due to the sudden sliding of a base isolated structure is studied. Shake table experiments were conducted using a scaled model of a single-bay three-story moment-resisting steel frame structure. Different base conditions, namely, a fixed base, sliding base and sliding base with conical spring cases were simulated alternatively. Two types of attached components were fabricated, namely, 1) components tuned to the second mode of the primary structure and 2) components tuned to the fundamental mode of the primary structure. Each of these two types of components was attached, one type at a time, to the first and third floor levels of the frame structure. Component response amplifications are then compared in case of sliding only and sliding with conical spring base condition with respect to the fixed based condition of the structure. The energy transfer phenomena due to sudden sliding of the structure were established by the short-term Fourier transform (STFT) analysis of the component response. Finally, the component response amplification factor with respect to the attached floor level is provided and compared with the provisions made in ASCE-7-05 [15].

2. Model Description

2.1 Structural Model

The experimental study considered a three-story single bay steel moment-resisting frame model as described by the schematic diagrams in Figures 1 and 2. The plan dimension of the frame was considered as 1000 mm × 900 mm with 1000 mm as its shaking direction and the elevation was considered as 1.75 m. The first story height of the frame was 0.75 m and the remaining two stories were 0.5 m each. The structural members were designed following the weak-beam strong-column design practice. The beams and columns of the model were square solid sections made up of mild steel with dimensions 10 mm × 10 mm and 12 mm × 12 mm, respectively. In order to simulate the floor masses two steel plates (10.4 kg each) were connected to each of the three floor levels. The plates were connected along the shaking direction using hooks in such a way that they do not contribute to the stiffness of the frame in the direction of shaking. The experiment was conducted for fixed, sliding and sliding with nonlinear spring base conditions as described in Figure 3.

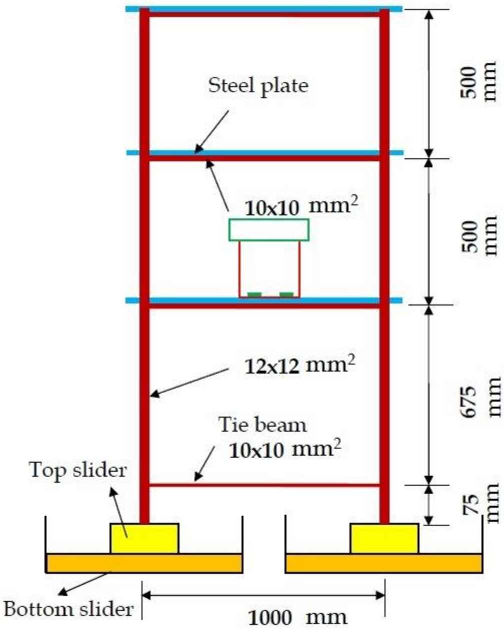

Figure 1: Schematic diagram of the model [10]

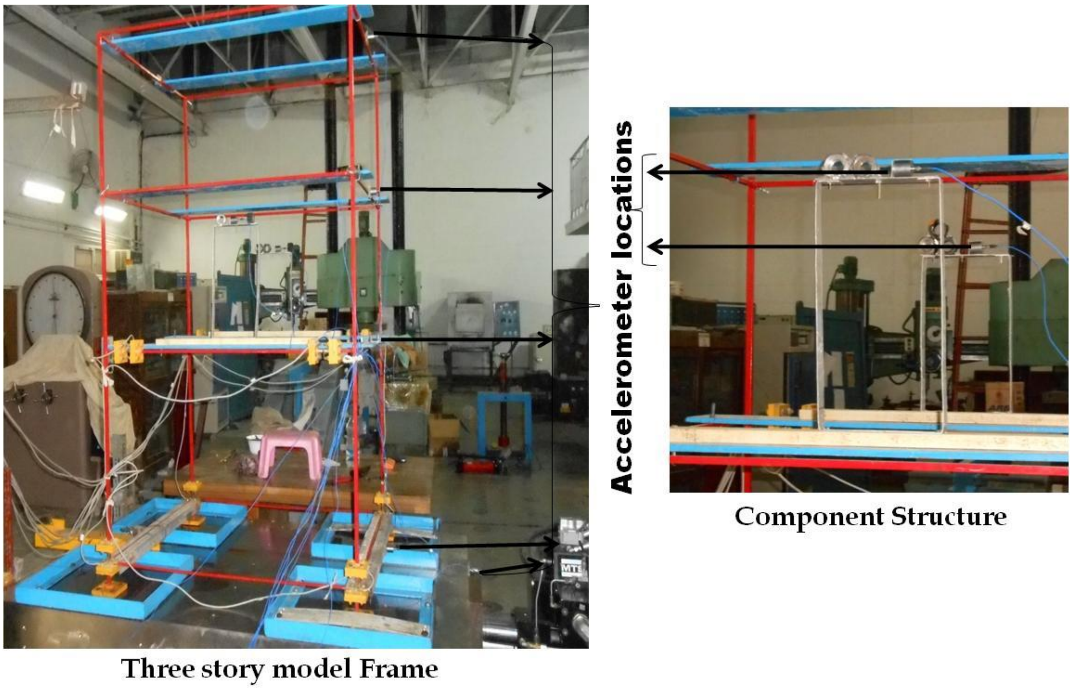

Figure 2: (a) Three story single bay steel moment-resisting frame model (c) Component structure

2.2 Base Isolation Model

The flat sliding bearing isolation system was used as one of the base conditions in the study. In order to model the sliding isolation system, each column was connected to a square steel plate of dimension 100 mm x 100 mm at its base and this plate behaved as the top slider. Four large steel base plates of dimension 450 mm x 380 mm were connected to a boundary frames which were rigidly attached to the shake table. These large plates worked as the bottom slider. On the top of these bottom sliders the base plates (top sliders) of the superstructure were placed.

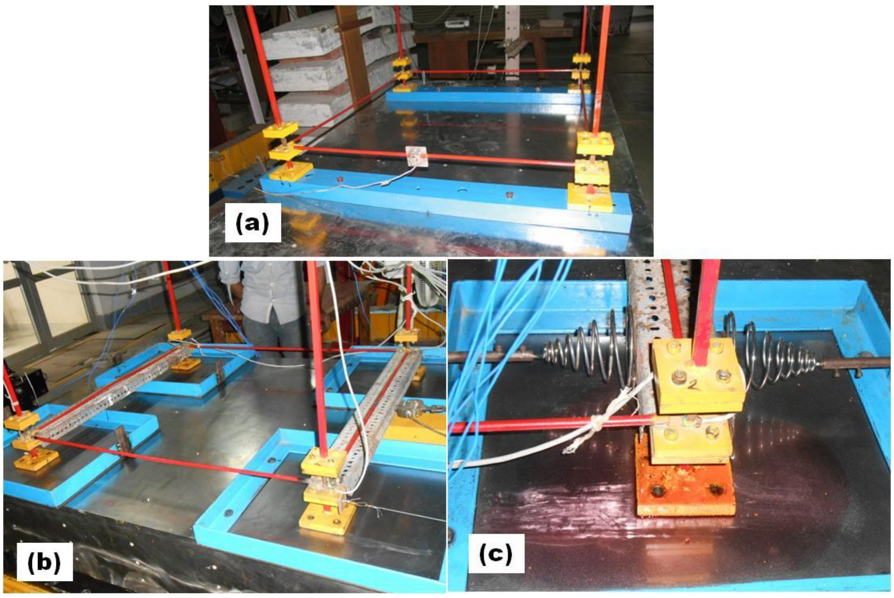

Figure 3: Photographs showing different base conditions [10] for (a) fixed base Model (b) sliding base model and (c) sliding base with nonlinear spring

Hence, the top slider was able to slide over the bottom slider whenever the lateral force in the ground column exceeded the frictional force between the two sliders. All column bases were connected together by circular ties of 10 mm diameter to provide equal degrees of freedom to all the column bases. These ties were placed at a height of 75 mm from the base as shown in Figures 1 and 2. The base plate bottom slider dimensions were considered from the analysis of the experimental model as simulated in OpenSees [10] using flat sliding bearing elements with coulomb friction model. Figure 3 b demonstrates the preparation of the sliding base condition of the model frame on the shake table.

Apart from the sliding only condition, flat sliding bearing coupled with nonlinear spring was considered as another base condition in order to introduce a restoring mechanism to the sliding only system. The nonlinear behavior was represented by a conical spring. Before sliding, structure provides stiff behavior. At the initiation of sliding, conical spring offers very low initial stiffness limiting the force transfer to the superstructure. Hence, the efficiency of the base isolation is achieved at a moderate intensity earthquake. At a further increase in base displacement, the spring stiffness increases significantly resisting the base displacement and thus, at higher intensity earthquakes, the conical spring becomes very effective in resisting the base displacement. Moreover, the restoring mechanism, which provides a re-centering force to bring back the structure to its original position, minimizes the residual displacement of the structure. Therefore, flat sliding bearing with conical spring shows an adaptive behavior at different intensities of earthquake. The conical spring dimensions, as finalized from OpenSees [10] analysis of the model, are demonstrated in Figure 4. Conical springs were loosely placed in an un-stretched condition on both sides of each column in the direction of shaking so that the largest loop of the conical spring was towards the column face. The other face of the spring was connected to the boundary frame, which was rigidly connected to the shake table. Thus, the spring behaved as a compression only member, which is necessary for keeping the initial stiffness of the sliding base isolation system low. Figure 3 c demonstrates the preparation of the sliding with conical spring base condition of the experimental model on the shake table.

2.3 Component model

In this study, two types of components, one with its natural frequency tuned to the second mode of the model frame (Type I) and the second with its natural frequency tuned to the fundamental mode of the model frame (Type II), were designed. The component was comprised of a 'U'-shaped frame. Provisions were made to firmly attach the base of the component with the steel plate surface (mass 10.4 kg) using anchor bolts. A plate with much higher stiffness as compared to the 'U' shaped steel frame was connected to the top of the frame so that the plate behaves as a rigid mass and the component frame behaves as a single degree of freedom (SDOF) system. A schematic diagram of the component is described in Figure 1. In case of Type I, two components, one with natural frequency slightly higher than the second modal frequency of the experimental frame model (Component IH) and another with natural frequency slightly lower than the second modal frequency of the experimental frame model (Component IL), were fabricated. Similarly, for Type II, two components with natural frequency slightly higher (Component IIH) and slightly lower (Component IIL) than the fundamental frequency of the experimental frame, were fabricated. The various dimensions and the masses of each of the components are described in Table 1. One may note that the mass of the components includes the self-weight of the component, the weight of the accelerometer and the weight of some additional masses, which were attached to the component in order to tune them to the experimental model frame. In case of component Type I, the 'U'-shaped frame was made up of stainless-steel plate of thickness 1.5 mm. An aluminum plate with much higher thickness than the 'U'-shaped frame was connected to the top of the 'U'-shaped frame so that the plate behaves as a rigid mass because of its higher stiffness as compared to the mild steel frame. Thus, the component frame behaves as a single degree of freedom (SDOF) system. In case of component Type II, 'U'-shaped frame was made up of aluminum of thickness 1.5 mm and a rigid aluminum plate is connected to the top as similar to the component Type I. It may be noted that the component was very stiff in the out-of-plane direction of the frame. The design of the component was finalized by modeling it in OpenSees [10].

Table 1: Component Properties

Type	Component name	Material	height h (mm)	width w (mm)	mass (gm)
Type I	Component IH	Steel	175	200	500
	Component IL		175	200	650
Type II	Component IIH	Aluminium	290	172	300
	Component IIL		350	175	400

3. Model Characterization

3.1 Dynamic characterization of model

In order to obtain the dynamic properties of the structure as well as component models, impact hammer tests were conducted. The instruments used for the test purpose were: (i) a PCB086D20 [14] type short-sledge impulse hammer (sensitivity of 0.23 mV/N), (ii) PCB393B04 [14] seismic, miniature (50 gm), ceramic flexural ICP accelerometer (sensitivity of 1V/g) for measuring acceleration response , and (iii) a 4-channel FFT Agilent 35670A Dynamic Signal Analyzer [13] for data acquisition. For testing of the structural model, hammer was mildly struck at the middle of the top story beam along the direction of the intended shaking of the frame. Floor level acceleration data were recorded along the direction of hit from each story and for each record, ten such hits were considered to collect the average frequency response function (FRF traces) and coherence information. Thus, the three FRF traces representing each floor were obtained from the experiment. Since the structure was quite flexible, the head of the hammer was selected to be of mild hardness. During the experiment, coherence values at the resonance points were found to be close to unity. To evaluate FRFs, force-exponential window (available in [11]) was used with appropriate setup. Initially the natural frequencies of the experimental frame model without any component were estimated from the Dynamic Signal Analyzer [11]. In case of component type 1, the masses of the components were adjusted in a way that the three natural frequencies of the combined system were obtained as 5.813 Hz, 6.125 Hz and 6.375 Hz, which were near the second mode frequency (7.75 Hz) of the model frame without component. Similarly, the masses of the type 2 components were adjusted to obtain three frequencies of the combined system (1.75 Hz, 1.813 Hz and 2.215 Hz) near the fundamental frequency of the of the model frame without component. The natural frequencies of the systems are shown in Table 2.

To extract information of dynamic characteristics from the recorded FRF data, a commercial software ME'scopeVES5.0 [12] was used. In order to analyze the FRF data, a wire frame model of the structure was created in the ME'scopeVES5.0 [12] software and the mode shapes and damping ratios were obtained by analyzing the recorded FRFs (using global polynomial curve fitting method). The damping ratios were obtained as 2.02%, 1.68% and 0.64% for the fundamental, second and third modes of the frame model. One may note that these damping ratios, as obtained from the experimental data analysis, were in good agreement to the code specified values of damping ratios for steel structure.

Table 2: Natural frequencies of the components

System	1st mode (Hz)			2nd mode (Hz)			3rd mode (Hz)
Bare model		1.94			7.75		15.062
Model with component type I		1.688		5.813	6.188	6.938	15.062
Model with component type II	1.75	1.813	2.215		6.563		15.062

3.2 Friction characterization:

In order to select the shake table input, evaluation of the coefficient of static friction between the top and bottom sliders is carried out prior to the dynamic testing of the structure with sliding isolators. A pull tests was conducted considering the structural model and a string pulley system. A detailed description of the string pulley test can be obtained from [10]. The average coefficient of static friction was found to be 0.23 from the five trials in the string pulley test.

3.3 Spring characterization:

In this study, the conical spring is assumed to be made of steel with shear modulus G = 8 x 10^{10} N/m^2. Figure 3c shows the photograph of the conical spring fabricated as a restoring mechanism along with the sliding isolator in the experiment. In fabricating the conical spring (Figure 4a), the total height (H_0) was considered to be 120 mm, the number of loops (N) was considered as 7, the larger diameter (D_f) was taken as 100 mm, the smaller diameter (D_s) was taken as 20 mm, and the wire thickness (D_t) was taken as 4 mm. The experimental force-deformation behavior of the conical spring during compression is obtained by the screw jack testing (Figure 4b). Figure 4c shows the force-deformation curve obtained for the conical spring. As can be observed from this graph, the curve is a multi-linear one, consisting of lines AB, BC, CD and DE, with increasing slopes. The detailed design philosophy and the experimental design of the dimensions of this particular conical spring can be found in [8] and [10], respectively.

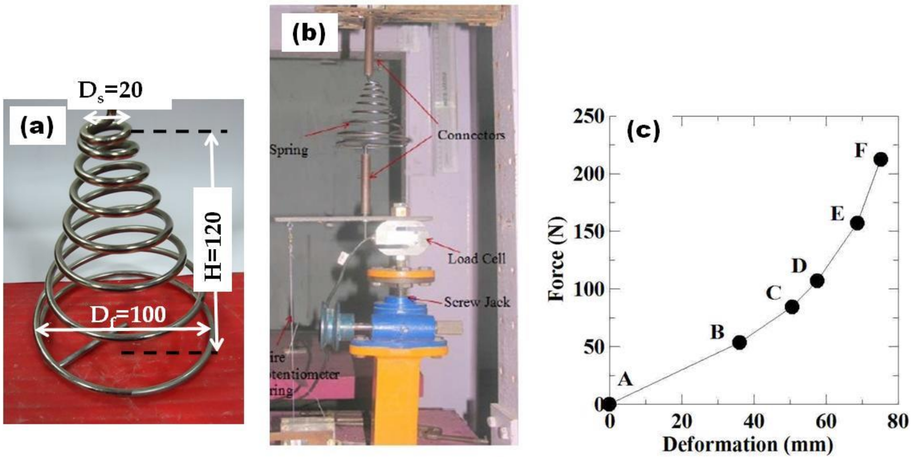

Figure 4: (a) Conical Spring description [10] (b) Screw jack testing for conical spring [10] (c) Force deformation behavior [10]

4. Dynamic testing

4.1 Shake table test

Experiments were conducted in the structural engineering laboratory, Indian Institute of technology Kanpur using a uni-axial shake table. The shake table has a platform of size 1.2 x 1.8 m and is driven by a 50 kN-150mm MTS computer-controlled servo-hydraulic actuator. The shake table has a displacement stroke of 7.5 cm and force capacity of 5kN.

4.2 Experimental setup

Tests were conducted for fixed base sliding base and sliding base with nonlinear spring base conditions as already demonstrated in Figure 3. A photograph of the shake table testing is shown in Figure 2a. Five accelerometers were used for measuring the acceleration at different points of the structure - three at the three different floor levels, one at the base of the structure and one on the shake table. In addition, two accelerometers were also mounted on two components to measure component responses. In order to measure the base movements of the structure with respect to the shake table (i.e., base sliding), two wire potentiometers were used, and one wire potentiometer was used at the top story. For testing of fixed base structure, instrument layout remained the same except that the wire potentiometers were removed. For recording acceleration as well as displacement data, NI PXI DAQ system [13] was used. Two components corresponding to a particular type (for example Component IH and Component IL) were simultaneously attached to one particular floor level during the test. Thus, two floor levels, first and the third were considered for the placement of the component. Each type of test was repeated three times for a particular ground motion. The responses of the primary structure and the component were considered as an average of the three trials.

4.3 Selected Ground Motion

The ground motions were considered in such a way that the behavior of the components attached to the model frame can be excited with different frequency ranges. Ground motions were considered from PEER strong motion database and from SAC ground motion (developed for the analysis of special moment resisting frames in Los Angeles area, USA). These motions were scaled depending on the displacement, velocity and acceleration capacities of the shake table although the displacement provided the dominant criteria for such scaling. The frequency contents of some of the motions were modified so that the peak amplitude of the response spectrum occurred near the fundamental period of the structural model. In order to select the ground motions from the database, time history analysis was carried out in OpenSees. Thus, five ground motions were selected from PEER strong motion database that showed peaks near the fundamental period of the model frame (i.e., 0.6 sec) and named as GM 1 to GM 5. These ground motions (GM 1—GM 5) were categorized as ground motion set 1. In addition, three ground motions (GM 6—GM 8) were considered from SAC ground motion database with dominant response near the second modal frequency of the model frame and were termed as ground motion set 2. The frequency of the ground motion set 2 was further scaled by factor 1.33 in order to increase the peak frequency. The detailed descriptions of the ground motions are demonstrated in Table 3.

Table 3: Detail of selected ground motion

Ground motion original	set	Modified name	Frequency scale	PGD (mm)	PGV (m/s)	PGA (g)
MORGANHILL	1	GM1	1.00	33.75	0.458	0.285
NORTHRIDGE	1	GM2	1.00	33.75	0.184	0.217
PARKFIELD	1	GM3	1.00	33.75	0.072	0.113
WHITTIER	1	GM4	1.00	33.75	0.179	0.230
CAPE-MENDOCINO	1	GM5	1.00	33.75	0.080	0.160
LA41	2	GM6	1.33	37.47	0.356	0.314
LA52	2	GM7	1.33	37.47	0.774	0.339
LA53	2	GM8	1.33	37.47	0.746	0.252

5. Results and discussion

In this paper the results as obtained from the experiment and associated discussions are primarily focused on the component responses attached to the main structure.

5.1 Component response

The component responses are obtained in terms of acceleration for all types of components attached to the first and third floor levels of the model frame. The ratio of the component acceleration between the sliding base and the fixed base cases are plotted along with the four component frequencies namely, 5.813 Hz (Component IL), 6.938 Hz (Component IH), 1.75 Hz (Component IIL) and 2.215 Hz (Component IIH) as shown in Figure 5. In the same figure, two vertical lines are also drawn for representing the fundamental and the second modal frequencies of the structural model frame. In the figure, two sets of ground motions are considered (Table 4) as described earlier. In case of ground motion set 1 (i.e., GM1 -- GM5), the responses for component Type I are amplified significantly, whereas the maximum amplification took place for Component IL (5.813 Hz) followed by Component IH (6.938 Hz), as can be seen from Figure 5a. However, the amplifications are not prominent for component Type II as can be observed from the figure. In case of ground motion set 2, no such amplification in the component responses are observed (Figure 5b), considering all the frequencies. The similar component response ratios as described for sliding only condition are obtained for the sliding with spring base condition as well for the component attached to the first floor-level. These ratios are presented in the same figure (Figure 5a and 5b) for the ground motion set 1 and 2, respectively.

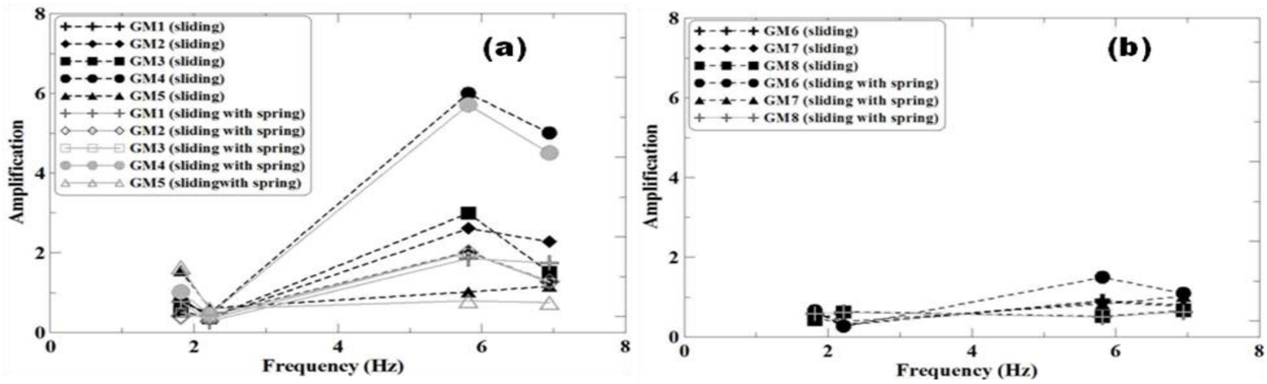

Figure 5: Ratio of component acceleration for base isolated conditions to fixed base condition at floor level 1 for: (a) ground motion set 1 and (b) ground motion set 2

In case of component attached to the third floor-level with sliding base condition, amplifications are observed (Figure 6a) for the component Type I, like the first floor-level, for ground motion set 1. However, as opposed to the first floor-level, amplifications are found to be dominant for the component with natural frequency 6.938 Hz (Component IH) as compared to the other component with natural frequency 5.813 Hz (Component IL). In case of component nearly tuned to the fundamental mode of the primary structure, no significant amplifications are observed. In case of ground motions set 2 (Figure 6b), a slight amplification is observed for the component with natural frequency 6.938 Hz. The similar component response ratios as described for sliding only condition are obtained for the sliding with spring base condition as well for the component attached to the first floor level. The ratios are presented in Figure 6a and 6b for ground motion set 1 and 2, respectively.

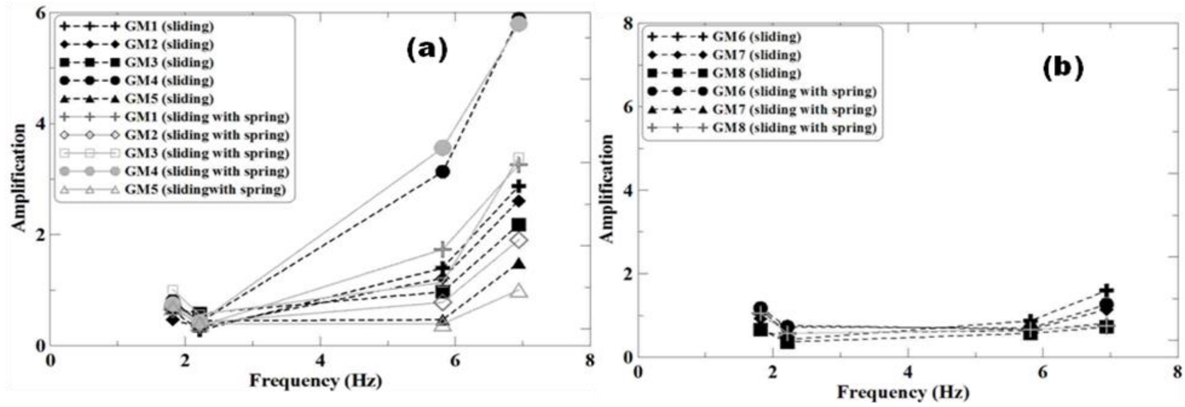

Figure 6: Ratio of component acceleration for base isolated conditions to fixed base condition at floor level 3 for: (a) ground motion set 1 and (b) ground motion set 2

5.2 Analysis of the result:

In order to understand the component response amplification, a short-term Fourier transform (STFT) of the component acceleration time histories are evaluated. Figure 7 demonstrates the STFT results for GM3, which belongs to ground motion set 1, considering the component attached to the first floor-level, for three different base conditions. It may be observed from the figure that both the fundamental and second mode frequencies are contributing significantly in the component response for fixed based structure (Figure 7b). However, in case of sliding only condition (Figure 7c), contribution of the second mode frequency is predominant. The excitation of the second mode occurs as the sudden jerk takes place when the base starts sliding. This can be ensured from the base displacement time history for GM 1 (Figure 7a). In case of sliding with nonlinear spring condition (Figure 7c), the contribution of the second mode is predominant. However, a partial contribution of the fundamental mode is also observed and thus, the relative excitation of the second mode can be considered as low in comparison to the sliding only case.

The STFT analysis clearly states that the sudden sliding causes transfer of energy among modes of the isolated system along with the energy dissipation. In ground motion set 1, the fundamental modes were excited initially since the response spectrum peaks occurred near the fundamental frequency of the structure. However, sudden sliding causes change in the stiffness of the system resulting into the transfer of energy to the higher modes from the fundamental mode. Consequently, the component tuned to the second mode gets excited causing amplification in response. This amplification reduces in case of sliding with nonlinear spring base condition that may be because of the gradual change in stiffness as compare to the isolated only condition.

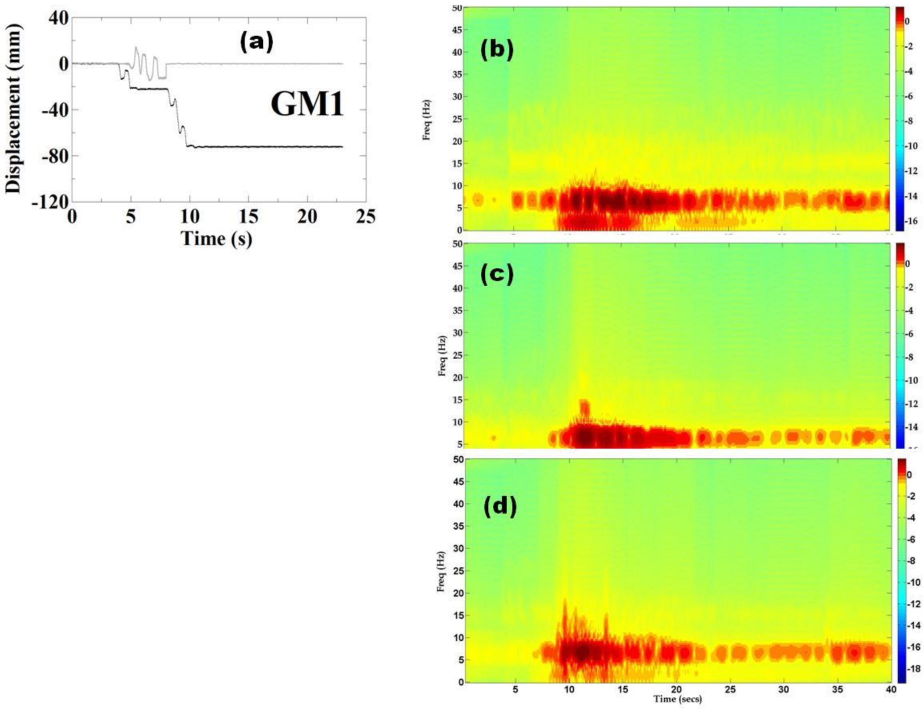

Figure 7: (a) Base displacement time history (b) STFT for fixed base condition, (b) STFT for the sliding only base condition and (c) STFT for sliding with spring base condition for GM 1

5.3 Amplification with respect to the attached floor

Table 4 represents the average amplification factors for the components with respect to the attached first floor level for sliding only and sliding with spring base conditions, considering two sets of ground motions namely, set 1 and 2, corresponding to two response spectrum peaks, respectively. Amplification is estimated for two component types, which are tuned to the 1st and 2nd modes of the structure as described in Table 2. The maximum amplification factor as specified in ASCE-7-05 [14] for the component design is 2.5. However, one may observe from the table that the amplification factor is significantly exceeding the code specified value for the component tuned to the second mode of the structure for all the cases. In case of ground motion set 1, having response spectrum peak near the fundamental mode of the structure, the sudden sliding causes the excitation of the second mode of the primary structure. Such excitation significantly amplifies the response of the component tuned to the second mode of the structure. In case ground motion set 2, the response spectrum have peak near the second mode of the structure, causing the amplification of the component response tuned to the second mode. In case of component tuned to the fundamental mode of the structure, the amplification is well inside the limit specified in ASCE-7-05 [14].

Table 4: Average component amplification with respect to the attached floor

	Componenr frequency (Hz)	Ground motion set 1 Component Amplification		Ground motion set 2 Component Amplification	
		Sliding only (g)	Sliding with spring (g)	Sliding only (g)	Sliding with spring (g)
Component tuned to the 1st mode	1.8	1.0	1.1	1.5	1.3
	2.2	0.9	1.2	1.7	1.3
Component tuned to the 2nd mode	5.8	5.8	6.8	8.3	8.6
	6.9	3.1	3.9	6.9	5.8

4. Conclusion

Shake table experiments were conducted with a scaled model of a single bay, three-story moment-resisting steel frame with attached components tuned to the 1st and 2nd modal frequency of the structure, under fixed, sliding and sliding with nonlinear spring base conditions. The effect of sudden sliding on the component structures at sliding only and sliding with spring base conditions are reported in this work. Following observations are made from this work:

a. The study demonstrates that a component housed in a base isolated structure may be more vulnerable seismically in comparison to the case when the component is housed to the same structure but fixed at its base. This will be of concern, if the component is attached to the lower floor levels of the building and the frequency of the component is close to the second mode frequency of the structure. This is because, in general, under seismic scenario the energy of the fundamental mode is the highest and as a result of sliding, part of this energy is transferred to the second mode of the structure.

b. The component acceleration with respect to the attached floor level acceleration is estimated for the two base isolated conditions namely, sliding base and sliding with spring base conditions. The results are compared with the component amplification factor with respect to the attached floor as provided in ASCE-7-05 [15]. It is observed that the amplification factor is significantly higher than the codal provisions for all the base isolated cases for the components tuned to the second mode. However, the amplification factor is within the specified limit in case of component tuned to the fundamental mode.

The experimental results thus establish the vulnerability of the non-structural component during a seismic event for a base isolated structure and emphasize the necessity to estimate the exact component response in such cases instead of considering the code specified amplification factor.

4. Acknowledgements

The authors would like to sincerely thank all the staff of Structural Engineering Laboratory, especially, Dr. K.K. Bajpai and Mr. Mohit Dwivedi for valuable help in conducting these tests. The project was funded by Department of Science and Technology (SERB/DST), Government of India. Any opinions and findings expressed in this paper are those of the authors, and do not necessarily reflect those of the funding agency.

5. Copyrights

6. References

[1] Villaverde, R. (2011): Recent advances in base isolation technology. *Sixth International Conference of Seismology and Earthquake Engineering*, Tehran, Iran (16-18 May 2011).

[2] Hamidi, M., El Naggar, M. H., Vafai, A., and Ahmadi, G. (2003): Seismic Isolation of Buildings with Sliding Concave Foundation (SCF). Earthquake Engineering and Structural Dynamics, 32(1), 15–29.

[3] Fenz, D. M. and Constantinou, M. C. (2007): Spherical Sliding Isolation Bearings with Adaptive Behavior: Theory. *Earthquake Engineering And Structural Dynamics*, 37, 163–183.

[4] Panchal, V. R. and Jangid, R. S. (2007). Variable Friction Pendulum System for Seismic Isolation of Liquid Storage Tanks . *Nuclear Engineering and Design*, 238, 1304–1315.

[5] Zayas, V. A., Low, S. S., and Mahin, S. A. (1987): The FPS Earthquake Resisting System; Experimental Report." Report no., Earthquake Engineering Research Centre, University of California

[6] Pranesh, M. and Sinha, R. (2000): VFPI: An Isolation Device for Aseismic Design. *Earthquake Engineering And Structural Dynamics*, 29, 603–627.

[7] Gluck, J., Ribakov, Y., and Dancygier, A. N. (2000): Selective control of base-isolated structures with cs dampers. *Earthquake Spectra*, 16(3), 593–606.

[8] Chakraborty, S., Roy, K., and Ray Chaudhuri, S. (2016): Design of re-centering spring for flat sliding base isolation system:theory and a numerical study. *Engineering Structures*, 126

[9] Chakraborty S, Ray Chaudhuri S. (2017): Energy transfer to high frequency modes of a building due to sudden change in stiffness at its base. ASCE, *Journal of Engineering Mechanics*, 143(8)

[10] Sachdeva, G., Chakraborty, S., Ray Chaudhuri, S (2018): Seismic response control of a structure isolated by flat sliding bearing and nonlinear restoring spring: Experimental study for performance evaluation *Engineering Structures*, 159

[11] OpenSees (2014): OpenSees – Open System for Earthquake Engineering Simulation. Pacific Earthquake Engineering Research Center (PEER), Richmond, California, USA (http://opensees.berkeley.edu/).

[12] Instruments, N. (2014). National Instruments Corporation, USA (http://www.ni.com/). ME'scopeVES (2013). ME'scopeVES5.0. Vibrant Technology Inc., 5 Erba Lane, Suite B, Scotts Valley, California, 95066.

[13] Agilent 35670A dynamic signal analyzer (2014) Keysight Technologies (http://www.keysight.com). Agilent Technologies, Santa Clara, California

[14] PCB (2013): PCB Piezotronics. PCB Piezotronics Inc, 3425 Walden Avenue Depew, New York, 14043-2495, USA. Technologies, A. (2013). Agilent. Agilent Technologies Inc, Santa Clara, California.

[15] American Society of Civil Engineers (2006): Minimum Design Loads for Buildings and Other Structures, ASCE-7-05

